Epidemic spread and bifurcation effects in two-dimensional network models with viral dynamics

Henry C. Tuckwell,* Laurent Toubiana, and Jean-Francois Vibert
Epidémiologie et Sciences de l'Information, University of Paris VI, INSERM U444, 27 rue Chaligny, 75571 Paris Cedex 12, France
(Received 6 March 2000; revised manuscript received 22 May 2001; published 26 September 2001)

We extend a previous network model of viral dynamics to include host populations distributed in two space dimensions. The basic dynamical equations for the individual viral and immune effector densities within a host are bilinear with a natural threshold condition. In the general model, transmission between individuals is governed by three factors: a saturating function $g(\cdot)$ describing emission as a function of originating host virion level; a four-dimensional array **B** that determines transmission from each individual to every other individual; and a nonlinear function F, which describes the absorption of virions by a host for a given net arrival rate. A summary of the properties of the viral-effector dynamical system in a single host is given. In the numerical network studies, individuals are placed at the mesh points of a uniform rectangular grid and are connected with an $m^2 \times n^2$ four-dimensional array with terms that decay exponentially with distance between hosts; g is linear and F has a simple step threshold. In a population of $N=mn$ individuals, N_0 are chosen randomly to be initially infected with the virus. We examine the dependence of maximal population viral load on the population dynamical parameters and find threshold effects that can be related to a transcritical bifurcation in the system of equations for individual virus and host effector populations. The effects of varying demographic parameters are also examined. Changes in α, which is related to mobility, and contact rate β also show threshold effects. We also vary the density of (randomly chosen) initially infected individuals. The distribution of final size of the epidemic depends strongly on N_0 but is invariably bimodal with mass concentrated mainly near either or both ends of the interval $[1,N]$. Thus large outbreaks may occur, with small probability, even with only very few initially infected hosts. The effects of immunization of various fractions of the population on the final size of the epidemic are also explored. The distribution of the final percentage infected is estimated by simulation. The mean of this quantity is obtained as a function of immunization rate and shows an almost linear decline for immunization rates up to about 0.2. When the immunization rate is increased past 0.2, the extra benefit accrues more slowly. We include a discussion of some approximations that illuminate threshold effects in demographic parameters and indicate how a mean-field approximation and more detailed studies of various geometries and rates of immunization could be a useful direction for future analysis.

DOI: 10.1103/PhysRevE.64.041918 PACS number(s): 87.10.+e, 05.40.−a, 02.50.−r

I. INTRODUCTION

In recent papers [1,2] we have considered new mathematical models for the spread of viral infection within human or other populations in which both the dynamics of viral (or bacterial) growth within individuals and the interactions between individuals are taken into account. In [1] the model was essentially deterministic whereas in [2] a stochastic model was introduced. In both of those papers the host population was considered to be distributed at discrete points on a line segment. Threshold phenomena were observed with respect to several parameters controlling the dynamics of viral growth and of immune system efficiency. In [2] a broad-based stochastic resonance effect was observed as the environmental viral noise parameter increased. In [3] heterogeneous spatial effects were taken into account in deterministic and stochastic SEIR frameworks. Our approach differs from classical SEIR or SIR models [3–6] or social network models [7], because in those the variable describing the state of the host as the amount of infection is discrete whereas ours is continuous. Furthermore, in the present approach different types of viruses may be distinguished in regard to their individual dynamical growth patterns as well as the various immune states of the individual hosts, giving a much more accurate representation of the procesess of growth and spread of the disease. Temporal and spatial patterns of drug treatment and vaccination may also be incorporated in such dynamical models. Furthermore, within a given viral type there are usually different strains that have differing properties of transmission and differing responses to such containment measures [8,9]. This aspect can be easily incorporated using the present approach with an additional index on the viral state variable.

II. DESCRIPTION OF MODEL

The individual hosts are assumed, for simplicity, to reside or be located at positions $x_{ij}, i=1, \ldots, m; j=1, \ldots n$, relative to some fixed rectangular coordinate system in the plane. Although these positions may be arbitrary, they are assumed throughout the numerical work that follows to be at the regular lattice points of a uniform rectangular grid. The (i,j) host has an effector population or density a_{ij} and a viral population or density v_{ij}, where these $2mn$ variables are all nonnegative. ''Effector'' is a blanket term covering many (complexly generated) immune system agents that lead to the elimination or annulation of the disease-causing virus or other noxious particles. In the general form of the model it is

*Corresponding author. Email address: tuckwell@b3e.jussieu.fr

 ©2001 The American Physical Society

assumed that the following differential equations govern the evolution of the system for given initial conditions:

$$\frac{da_{ij}}{dt}=\lambda_{ij}-\mu_{ij}a_{ij}+\epsilon_{ij}a_{ij}v_{ij}, \tag{1}$$

$$\frac{dv_{ij}}{dt}=r_{ij}v_{ij}\left(1-\frac{v_{ij}}{k_{ij}}\right)-\gamma_{ij}a_{ij}v_{ij}+F\left[\sum_{i'}\sum_{j'}\beta_{i'j',ij}g(v_{i'j'})\right]. \tag{2}$$

The parameters have the following meanings for individual (i,j): λ_{ij} is the rate of production and/or transport of effectors, μ_{ij} is the death (clearance) rate of effectors, ϵ_{ij} is the rate of production of effectors in response to a unit viral population, r_{ij} is the intrinsic growth rate (measure of ''virulence'' and referred to as the virulence parameter) of the viral population, k_{ij} is the saturation value of the viral population, and γ_{ij} is the clearance rate of virus particles. The quantities $\beta_{i'j',ij}, i',i=1,\ldots,m;\ j',j=1,\ldots,n$ are the viral transmission rates from individual (i',j') to individual (i,j). $F(\cdot)$ is a possibly nonlinear function that incorporates the ability of the target individual to absorb virions when they arrive at a certain rate. This could also depend on (i,j) but is assumed to be the same for all individuals. The amount of virus emitted from the host (i',j'), when his viral level is $v_{i'j'}$, is $g(v_{i'j'})$. It is likely that in reality g is an increasing yet saturating function of its argument, such as $g(x)=1-e^{-x}$ in scaled form. Thus in summary the general form of transmission process has three components: g describes the amount emitted from any host; the quantities $\beta_{i'j',ij}$ determine the rate of transmission of the emissions to other hosts; and F determines the amount absorbed into a target host.

Simplifications in the numerical work

In the numerical work we have made the strength of transmission between individuals an exponentially decaying function of the distance between them with

$$\beta_{i'j',ij}=\beta(1-\delta_{i'j',ij})\exp[-\alpha\sqrt{(i'-i)^2+(j'-j)^2}], \tag{3}$$

where $\delta_{i'j',ij}=1$ if $i'=i$ and $j'=j$ but is otherwise zero. This incorporates a truly spatial effect and represents an averaging of the effects of various members of the community on one another, as the distances between them fluctuate. Furthermore, the function g has been taken as linear, which should be accurate at small and modest virion densities. The function F has been assigned a threshold value such that $F(x)$ is zero for arguments less than a critical value, as described fully in Ref. [1]. That is, we may put $F(x)=H(x-x_{\rm crit})$, where $x_{\rm crit}$ is the critical rate at which virions must arrive at an uninfected individual in order to instigate a sustained infection. The value of k_{ij} has been set at infinity. Thus Eq. (2) becomes simply

$$\frac{dv_{ij}}{dt}=r_{ij}v_{ij}-\gamma_{ij}a_{ij}v_{ij}+F\left[\sum_{i'}\sum_{j'}\beta_{i'j',ij}v_{i'j'}\right]. \tag{4}$$

III. THE VIRAL-EFFECTOR SYSTEM IN ONE INDIVIDUAL

The properties of the above viral network clearly depend both on the individual dynamical responses to the arrival of virions and to the manner in which the populations of virions within individuals are connected. It is therefore useful to consider in some detail the properties of the viral-effector system in one individual. Indeed, it will be seen that a considerable part of the network behavior is explained by such a consideration of the corresponding system for one individual. The latter is simply

$$\frac{da}{dt}=\lambda-\mu a+\epsilon av, \tag{5}$$

$$\frac{dv}{dt}=rv-\gamma av, \tag{6}$$

and has been analyzed in detail, along with various models for human immunodeficiency virus-1, in Ref. [10]. Note that the case $\lambda=0$ gives the classical Lokta-Volterra system [11]. There are two critical points, $P_1=(\lambda/\mu,0)$ and $P_2=(r/\gamma,[\mu r-\lambda\gamma]/\epsilon r)$. The eigenvalues associated with P_1 are $\lambda_1=-\mu$ and $\lambda_2=r-(\lambda\gamma)/\mu$. If $\lambda=0$, then $\lambda_1=-\mu$ and $\lambda_2=r$ so that the critical point is an unstable saddle point. If $\lambda\neq 0$, then P_1 is an unstable saddle point if $\lambda\gamma\leqslant r\mu$ and an asymptotically stable node if $\lambda\gamma>r\mu$. The eigenvalues associated with P_2 are

$$\lambda_{1,2}=-\frac{1}{2r}\{\gamma\lambda\pm\sqrt{(\gamma\lambda)^2+4r^2(\gamma\lambda)-4\mu r^3}\}.$$

If $\lambda=0$ the eigenvalues are $\lambda_1=-i\sqrt{\mu r}$ and $\lambda_2=i\sqrt{\mu r}$, so that P_2 is a center. If $\lambda\gamma>\mu r$, then $\lambda_1<0<\lambda_2$ so that P_2 is an unstable saddle point. If $\lambda\gamma<\mu r$, then there are two distinct possibilities: (a) $4r^2/(\lambda\gamma)^2[\mu r-\gamma\lambda]\leqslant 1$. In this case, the eigenvalues are distinct and negative, which makes P_2 an asymptotically stable node; (b) $4r^2/(\lambda\gamma)^2[\mu r-\gamma\lambda]>1$. The eigenvalues are then a complex conjugate pair with a negative real part. Hence P_2 is an asymptotically stable spiral point.

Now, if $\lambda\gamma>\mu r$, the point P_2 occurs at negative v and hence is not at a biologically relevant value. There is then just one meaningful critical point P_1 on the a axis and this is an asymptotically stable node. Thus no matter where solutions start in the non-negative quadrant, they end up at P_1 with zero virions and with $a(\infty)=\lambda/\mu$ effectors. On the other hand, when $\lambda\gamma<\mu r$, there is an unstable saddle point on the a axis at P_1 together with an equilibrium point P_2 in the positive quadrant that is either an asymptotically stable node or an asymptotically stable spiral point. Then whenever the initial value $v(0)$ is positive, regardless of whether $a(0)$ is positive or zero, the system ends up at P_2. Thus in such cases it is impossible to end up with zero virions; an equi-

librium is reached with r/γ effectors and $(\mu r-\lambda\gamma)/\epsilon r$ virions. If λ is relatively small, the solutions undergo damped oscillations on their approach to P_2; if λ is large enough solutions show no oscillatory behavior and proceed directly to P_2. At the critical value $\lambda\gamma=r\mu$ where there is a change of stability of P_1 and P_2, the two critical points coincide, both being located at $(\lambda/\mu, 0)$ with P_2 emerging as the asymptotically stable steady state for $\lambda/\mu<r/\gamma$. Thus, there is a *transcritical bifurcation*, with P_2 emerging as λ/μ decreases below r/γ. This transcritical bifurcation plays a key role in understanding some of the threshold effects that will be seen below in the numerical results.

IV. NUMERICAL RESULTS FOR THE NETWORK

In the numerical work, the standard set of immune and viral parameters are assumed to be the same for each individual. These values are based approximately on those that could be found for the influenza virus as explained in [1]: $\lambda=0.5$, $\mu=0.05$, $\epsilon=0.01$, $r=1$, and $\gamma=0.1$. This choice is at the bifurcation point for one individual so that $P_1=P_2$. We distinguish the above parameters, which are called dynamical system parameters, from the following two parameters, which are called *demographic parameters* and which completely describe the four-dimensional array $\beta_{i'j',ij}$. These two parameters are: α, which determines the spatial range of an infected host's emitted virions; and β, which measures the mean contact rate of individuals. Since a large value of α implies limited influence, the reciprocal of α can be used to quantify the *mobility* of the individuals in the sense of how far they travel within the population. Thus the model is more versatile than ones in which contact is restricted to nearest neighbors only as in [12].

A. Dynamical system parameters

There are five intrinsic dynamical system parameters λ, μ, ϵ, r, and γ; and the superimposed dynamical parameters v_c, the threshold virion level for viral growth in any host and the starting value $v(0)$ of that growth [1]. The latter two parameters are kept fixed throughout this article. We first show in Fig. 1(a), the maximum mean virion level

$$\overline{v}_{\max}=\max_{t\geq 0}\frac{1}{N}\sum_i\sum_j v_{ij}(t)$$

across the population versus the effector source parameter λ that is a measure of the tone or state of the host immune system. These results are based on one trial for each λ with the same initial configuration of 40 infected individuals, randomly chosen in a population on a square 40 by 40 lattice at a rate therefore of 2.5%. It can be seen that for values of λ greater than 0.35, the degree of viral growth and spread is relatively very small. As λ decreases through 0.35, there occurs a sharp increase in the overall viral level throughout the population with a rapid rise until $\lambda=0.46$ and further decreases result in a steady rise in maximum mean virion level. The threshold effect is explicable in terms of the transcritical bifurcation in the effector-virus system for one individual

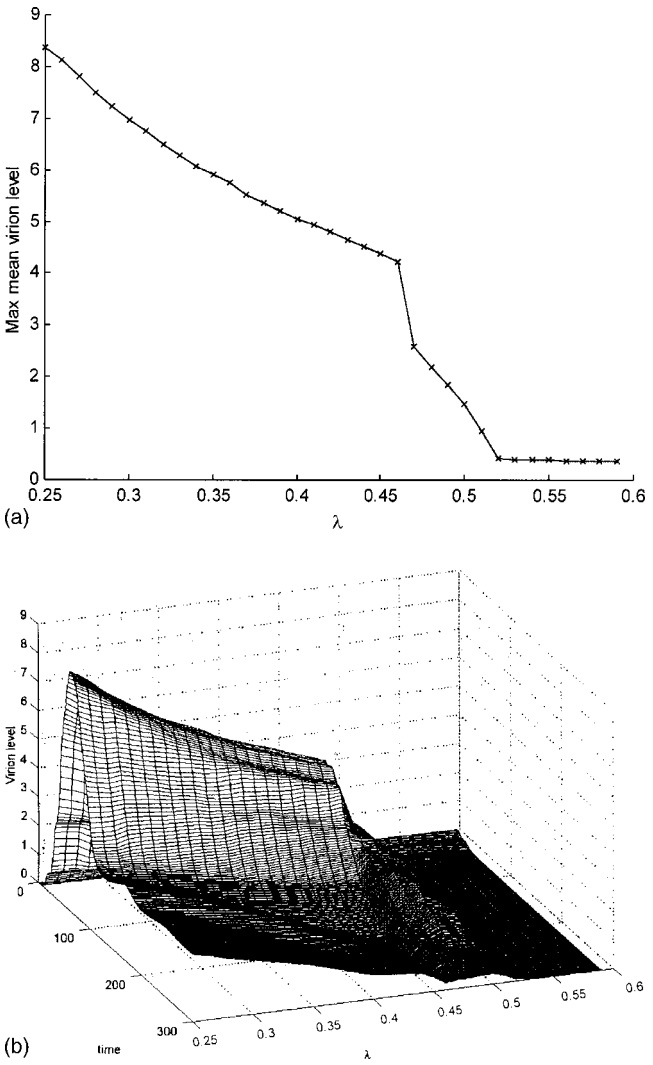

FIG. 1. (a) The maximum mean virion level across the population in one trial as the immune parameter λ varies. The remaining parameter values are the standard set—see text. Based on influenza data, units of time are approximately 5 h and for virus particles approximately 10^{11}/ml of infected tissue. (b) Three-dimensional representation of the time courses of the mean virion level across the population for various λ, from which are extracted the maxima shown in Fig. 1(a). The actual values of λ and the units are as in Fig. 1(a).

that, with the parameters used here, occurs in fact at $\lambda=0.5$. For the network, the change point is slightly displaced in the direction of larger values of λ. In individuals the orbits are qualitatively different on either side of the bifurcation point. For large λ, the steady state is with zero virions whereas for values of $\lambda<0.5$, the final approach is to a critical point with a positive virion level.

The actual time courses of the mean virion density across the population in one trial, $\overline{v}(t)=(1/N)\Sigma_i\Sigma_j v_{ij}(t)$, for various λ are shown in the three-dimensional plot of Fig. 1(b). One can see clearly the differences in the trajectories on either side of the bifurcation point for the viral-effector system in one individual. At the smaller values of λ there are apparent slow and gentle oscillations in $\overline{v}(t)$ that may reflect

the oscillations in the individual host viral levels, though the latter are not expected to be synchronized. These results were obtained with the remaining intrinsic dynamical system parameters μ, ϵ, r, and γ, at fixed values as given above. For different sets of values of these other parameters, the approximate threshold value of λ is, based on the birfurcation analysis for an individual, $\lambda_c = \mu r/\gamma$. There is no dependence on ϵ, but this parameter determines the overall magnitude of the individual, and hence population, virion level through the asymptotic value of $v_{ij}(t)$ at the equilibrium point $P_2 = (r/\gamma, [\mu r - \lambda\gamma]/\epsilon r)$.

Results obtained when r was varied from the standard value of unity show a similar sharp threshold effect as was found in [1] in one space dimension. This can be seen in Fig. 2(a), where the mean maximum virion level is plotted for values of r from 0.5 to 1.5. The threshold effect is seen to be sharper than that for λ, which implies a greater sensitivity to this parameter with respect to the degree of invasion of the host population. Now, since it is possible that the number of infected hosts could be large even with a small mean maximum virion level, we have examined also the distribution of the final size X_F of the epidemics that ensue for various values of r on either side of the critical value $r_c \approx \lambda\gamma/\mu = 1$. In Fig. 2(b) we show the histograms of the total numbers of infected individuals with the values of $r = 0.90$, 0.97, 1.00, and 1.02. Here, 50 trials were performed for each value of r with randomly assigned configurations of 40 initially infected individuals. All other parameters were held at the standard values. It can be seen that the nature of the distribution of X_F is very different for these four values of r. With $r = 0.9$, the distribution is fairly tightly concentrated at values less than 100; for $r = 0.97$ the distribution is somewhat more spread out and fairly uniformly concentrated at values less than 200; then at $r = 1.00$ a very different situation ensues with all the mass concentrated at large values between 1200 and 1600; and finally, with $r = 1.02$, there is no mass except at the maximum value of $X_F = N = 1600$. The variation with respect to changes in r is further highlighted in Fig. 2(c). Here the mean value of X_F is plotted against r for many values of r on either side of r_c. There is a very abrupt increase in $E(X_F)$ near $r = 1$. Furthermore, it can be seen by comparing Figs. 2(a) and 2(c) that as r increases beyond 1.02, $E(X_F)$ does not (cannot) increase even though the maximum mean virion level is still increasing. This difference arises because the term *infected* does not distinguish degrees of infection. Results obtained by varying the remaining dynamical system parameters are not reproduced here. Rather, we proceed to an examination of the effects of changes in what we call demographic parameters as these are more pertinent to network effects.

B. Demographic parameters

We will first ascertain the quantitative effects of changes in the parameter α, which determines the extent of the spatial spread of viruses from any infected individual, and which we call the mobility parameter—large values of α corresponding to small mobility. Figure 3 shows a three-dimensional plot of the size of the epidemic, as measured by the total number of hosts that are touched by the disease (virus) throughout the time course of the numerical experiment. The two independent variables in this figure are α and the initial number N_0 of infected individuals in a total population of $N = 1600$. For each of the 49 combinations of N_0 and α, 40 trials were performed, with a randomly chosen initial configuration of infected hosts. The mean size of the epidemic obtained shows for each value of N_0 a relatively abrupt threshold as α decreases (i.e., mobility increases). For the values of N_0 used here, the critical value α_c lies between 0.8 and 0.85, and is a slowly increasing function of N_0. Thus when $N_0 = 10$, we have $\alpha_c \approx 0.8$, whereas when $N_0 = 40$, we have $\alpha_c \approx 0.85$. This behavior is easily accounted for by observing that a large epidemic may occur even if the density of initially infected individuals is small, providing the mobility of individuals and hence their domain of influence is large (small α).

We have also varied the demographic parameter β, which reflects the frequencies of collision between individual hosts. As indicated by the analysis below, this parameter shows a threshold effect. This can be seen by inspection of Figs. 4(a) and 4(b). In the first of these figures we see a three-dimensional plot of population mean virion level (one trial) vs time for various values of β. Many values were employed near $\beta = 0.01$ to examine any fine structure that might exist in the neighborhood of that value. In each of these simulations, the same initial configuration of infected hosts is employed. It can be seen how very differently the system behaves as β decreases away from 0.01. At the latter value a rapid and large upsurge occurs in the population virion level followed by an at first rapid, then relatively slow, decay phase. With not very much smaller contact rates there are a few undulations in virion level but these have small and decreasing amplitudes and it could be said that no epidemic occurs. These phenomena are further highlighted in Fig. 4(b) where we plot two properties of the population response against β, now on a linear scale. The solid curve shows the maximum population mean virion level whereas the dash-dot curve gives the time (divided by 10) at which the maximum was attained. An almost discontinuous change in the time to maximum occurs just to the left of $\beta = 0.01$, whereupon this quantity declines at first rapidly then slowly as the contact rate increases.

The final demographic parameter we have varied is the number N_0 of initially infected individuals; the distribution of such individuals is always assumed in the simulations to be random across the population. Of primary interest is the form of the probability distribution of the final size of the epidemic so in Fig. 5(a) we show the histograms of this random variable for various values of N_0 obtained from 50 simulations. When the initial fraction of infected individuals is very small at 0.0625% with $N_0 = 10$, the distribution of final sizes is concentrated at small values with a small amount of mass between about 1000 and the maximum number (recall $N = 1600$). With a relatively small increase to $N_0 = 15$, half of the mass is at very small sizes and we see that the probability of a major outbreak is roughly 0.5. When $N_0 = 20$, so that slightly more than 1% of the population is initially infected, the probability of a significant epidemic is

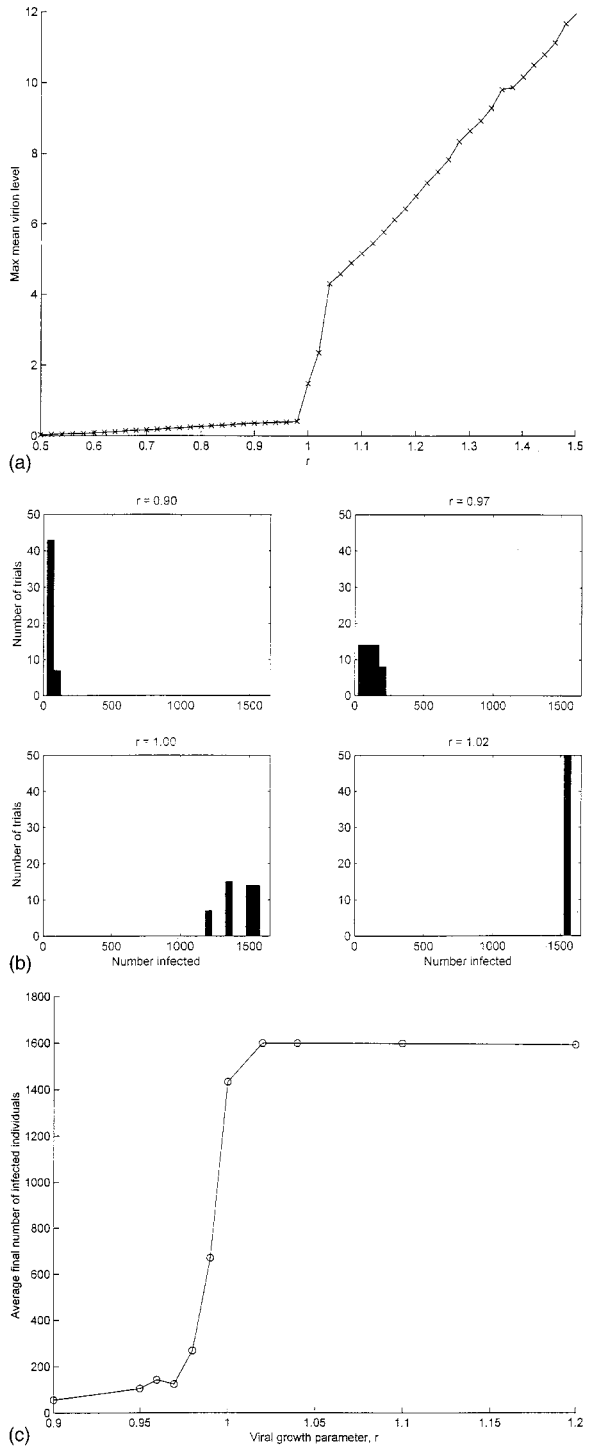

FIG. 2. (a) The maximum mean virion level across the population in one trial as the viral growth rate parameter r (per unit time) varies. The remaining parameter values are those of the standard set. Units of time are approximately 5 h and for virus particles approximately 10^{11}/ml of infected tissue. (b) Histograms of total numbers X_F of infected individuals for various values of the viral growth rate parameter r (per unit time), so chosen to lie on either side of the critical (bifurcation) value. Histograms obtained from 50 trials with random assignments of 40 initially infected individuals in a total population of 1600. (c) Mean value of X_F plotted against r (per unit time). Same set up as in Fig. 2(b) but with more data points.

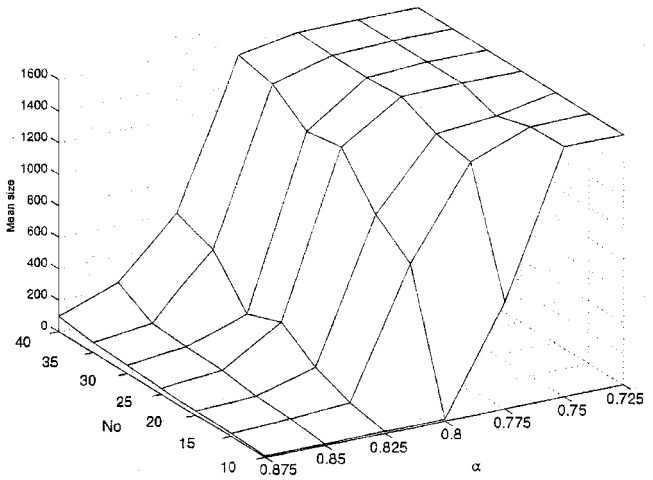

FIG. 3. Three-dimensional representation of mean final size, $E(X_F)$, of the epidemic as the initial number of infected individuals (N_0) and the mobility parameter (α, dimensionless or per unit distance between individuals) vary. Results based on 40 trials for each of the values of N_0 and α.

increased to about 0.75 and when $N_0=40$, a major event is certain and in fact the probability is close to one that nearly the entire population will be infected. For a more complete set of values of N_0, the mean final size of the infected population is shown plotted against this variable in Fig. 5(b). The increase in mean size is fairly smooth and saturating with no threshold effect. The saturation point at which increases in N_0 cause no further increase in mean epidemic occurs at about $N_0=60$. That is, if a critical mass of about 3.75% or more of the population is infected initially, then the entire population will end up being infected. However, it must be borne in mind that this result is based on nonstochastic dynamics, the only random component in the present analysis being in the choice of the initially infected individuals. When N_0 is small, the only factor (here) that determines whether or not a major outbreak occurs is the pattern of the geometrical arrangement of the initially infected hosts.

C. Effects of immunization

A very important aspect of the theory of epidemics is the effectiveness of programs of immunization. Extensive field monitoring programs are in progress to aid in an assessment of the results of patterns of influenza vaccination [13]. As is well known, some such programs have been very successful in eliminating or nearly eliminating some diseases, such as poliomyelitis and smallpox. Within the framework of a spatial model that includes both effector and viral dynamics, there are several ways in which one could attempt to ascertain the effects of immunization. We have chosen to represents an immunized individual as one who has on a prior occasion encountered the virus pertinent to the disease under consideration. We assume therefore that the effector level in an immunized host is equal to the equilibrium value that would have been attained had the virus run its course of growth and equilibration in that individual. With the standard set of parameters this means that if individual (i,j) is immunized, then $\alpha_{ij}(0)=\lambda/\mu=10$ since we assume that orbits

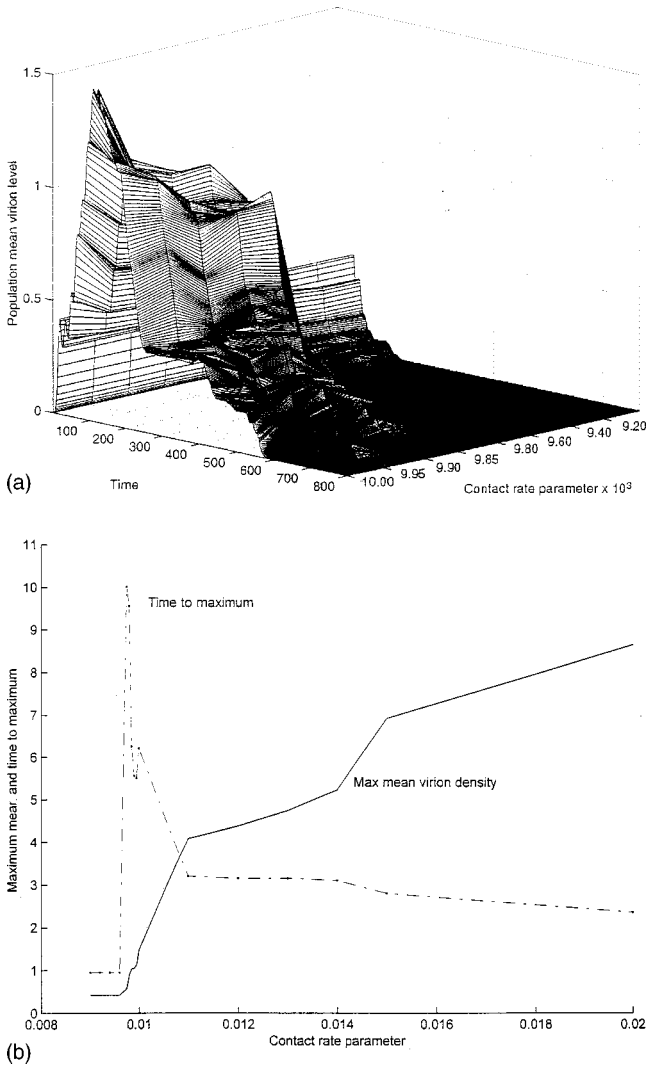

FIG. 4. (a) Mean population virion level plotted against time and contact rate parameter β (per unit time). Units of time and virion level here and in Fig. 4(b) as in Figs. 1(a) and 1(b). (b) Maximum population mean virion level (solid curve) and time (divided by 10) to maximum (dash-dot curve) vs contact rate parameter β (per unit time).

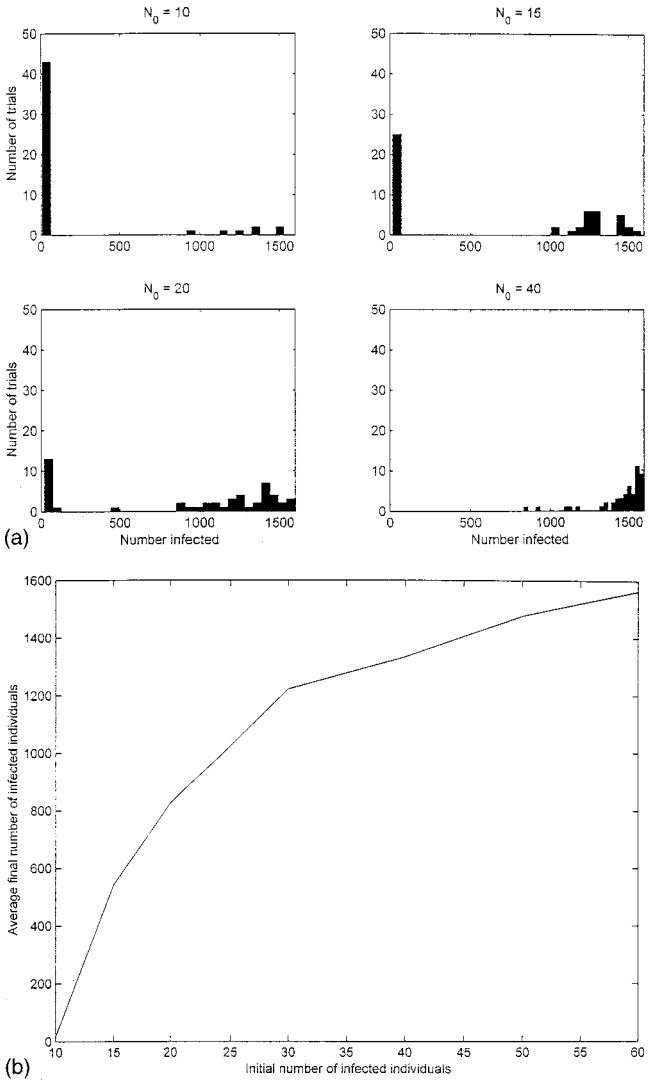

FIG. 5. (a) Histograms of final size of epidemic for four values of N_0, the initial number of infected individuals. In each case 50 trials were performed. (b) Showing the mean final size vs N_0, for a broad range of number of initially infected individuals.

end up at P_1. We thus chose, as in the previous simulations, a random selection of $N_0=40$ initially infected individuals. We call the immunization rate ρ and let this be the rate of immunization of the individuals who are not initially infected. Thus, since immunized individuals are protected, they are excluded when we determine the infection rate of the remaining $S=(N-N_0)(1-\rho)$ susceptible individuals and express this as a percentage. The results for the 50 simulations with each immunization rate are shown in Figs. 6(a) and 6(b). The histograms of the percentage infected for six values of ρ from 0.02 to 0.4 are shown in Fig. 6(a). The transition from low to high immunization rate is smooth with nearly all the mass at unity when the immunization rate is negligible and nearly all the mass near zero when the immunization rate is 0.4. The mean of such distributions is plotted against ρ in Fig. 6(b). Again one sees a fairly smooth dependence on ρ, the form of the curve being almost linearly decreasing for values of ρ from 0 to 0.2.

V. APPROXIMATIONS AND A MEAN-FIELD APPROACH

The mathematical model considered here for the spread and growth of a virus throughout a population of hosts differs qualitatively from previous approaches. For example, in early lattice models of epidemic spread [14] and in more recent SIR automata network models [15], the set of states available at each lattice point is discrete and finite. The present model gives the states of the individuals as solutions of coupled systems of differential equations. In [14] and [15] a mean-field approach has been used in order to estimate long term behaviors of the networks, especially if there exists a unique steady state. An attempt at a similar approximation with the epidemic network model with viral dynamics described herein proceeds by assuming that each individual is not far from the mean for the system. That is,

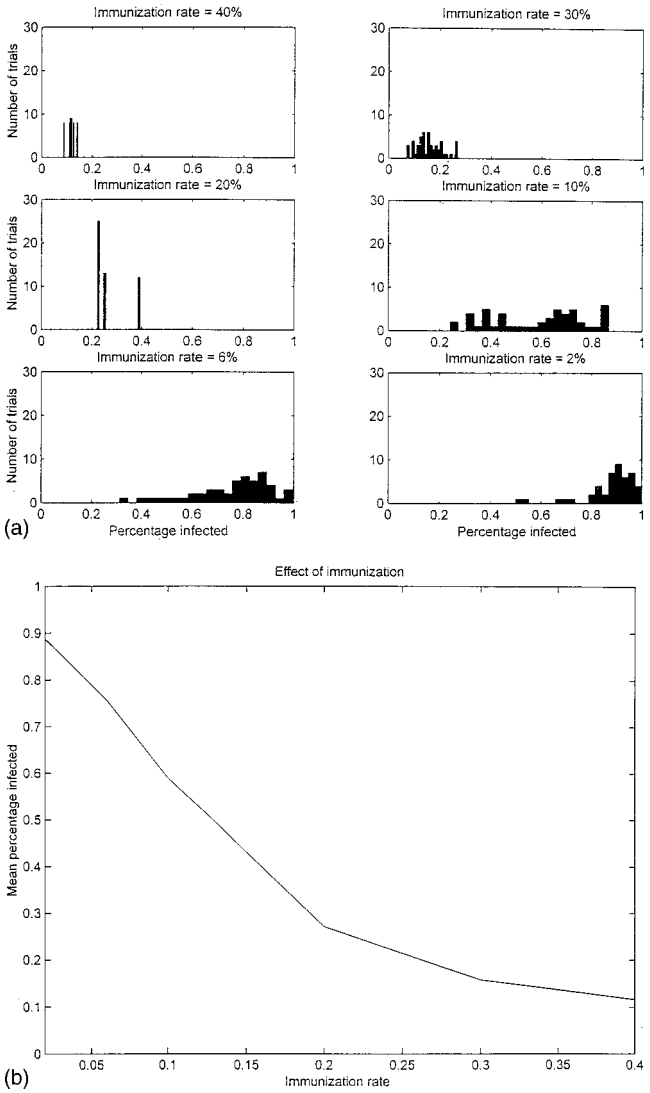

FIG. 6. (a) Histograms of percentage (of those who could be infected) of finally infected individuals for various immunization rates, ρ (dimensionless). (b) Mean percentage (of those who could be infected) of finally infected individuals plotted against immunization rate ρ (dimensionless).

the a_{ij} and v_{ij} can be replaced by the average values $\overline{a}$ and $\overline{v}$ across the population. This may be expected to be approximately valid if the transmission of virus between members of the population is rapid. The latter occurs if the mobility of individuals is high that implies that the parameter α is close to zero. In such a case we have approximately

$$\frac{d\overline{a}}{dt} = \lambda - \mu\overline{a} + \epsilon\overline{av}, \tag{7a}$$

$$\frac{d\overline{v}}{dt} = [r + \beta(N-1)]\overline{v} - \gamma\overline{av}, \tag{7b}$$

where N is the total number of infected and uninfected individuals. Initial behavior may be studied by replacing N by N_0. The system (7a) and (7b) is easily solved numerically with a Runge-Kutta method.

The threshold effect as α varies can be explained, heuristically, as follows. For simplicity, consider the one-dimensional model [1,2], with a linear emission function g so that

$$\frac{dv_i}{dt} = r_i v_i - \gamma v_i a_i + \beta \sum_j v_j e^{-\alpha|i-j|}. \tag{8}$$

If α is not too small, the dominant contributions to the sum in Eq. (8) are from the nearest neighbors so that, provided individual i is not at the edges of the population,

$$\frac{dv_i}{dt} \approx r_i v_i - \gamma v_i a_i + \beta e^{-\alpha}[v_{i-1} + v_{i+1}].$$

Further argument that v is roughly continuous in the sense that neighbors have approximately similar virion levels, leads to

$$\frac{dv_i}{dt} \approx [r_i + 2\beta e^{-\alpha}] v_i - \gamma v_i a_i .$$

This expression makes it evident that changes in the demographic parameters α and β are essentially effective changes in the viral intrinsic growth rate parameter r. Hence, if with a given r the system is near a bifurcation point, then changes in α and β may push the system to the other side of the bifurcation point. Thus, such changes in α and β may lead to similar threshold phenomena as are found when r itself is varied.

VI. CONCLUSIONS

A complete quantitative study of epidemics involves demographic components, which reflect properties of the host population and components that describe the dynamics of the invading organisms that are usually either virus particles or bacteria. Most of the previous studies have omitted the second of these components, as in the family of SIR or SEIR models. It is also necessary to include spatial distributions of hosts, which may be done via partial differential equations of the diffusion type [16], or as integrodifferential equations [1] or in a discrete framework as employed in this paper. We have considered here a two-dimensional Cartesian system of hosts whose viral populations interact with one another via contact and transmission. The properties of the dynamical system describing the viral-effector system are very influential in determining the magnitude and time course of outbreaks of disease, and for this reason we have included a brief analysis of the virus-effector system in a single individual. Most relevant is the occurrence of a transcritical bifurcation that gives rise to threshold effects as effector and viral parameters change. In particular, we have determined the temporal evolution of the population virion level and the distribution of the total numbers of infected individuals as parameters vary on either side of the bifurcation. We have also examined these quantities as certain demographic parameters, such as contact rate, mobility, and the number of initially infected individuals change. Finally we have examined how immunization rate affects the final size of the epi-

demic. We have found that the greatest benefit is obtained when the immunization rate increases up to 20%, with diminishing returns for further increases. In future work geometric effects in two and three space dimensions should be explored in detail, especially with respect to the effects of patterns and spatial rates of immunization. Of particular interest will be simulation with varying densities of population, representing cities, possibly as dynamical systems themselves, towns, villages, and countryside as well as the inclusion of age structure and mobile hosts. A mean-field study, as alluded to in the preceding section, may also be useful in order to obtain analytical results concerning the general effect of viral spread without specific regard to exact spatial configurations. Such an analysis has been carried out for many of the lattice models in [14] and [15].

ACKNOWLEDGMENT

H.C.T. appreciates the support of Institut National de la Santé et Recherche Medicale, Paris, and the hospitality at Alain-Jacques Valleron's unit 444.

[1] H. C. Tuckwell, L. Toubiana, and J-F. Vibert, Phys. Rev. E **57**, 2163 (1998).
[2] H. C. Tuckwell, L. Toubiana, and J-F. Vibert, Phys. Rev. E **61**, 5611 (2000).
[3] A. L. Lloyd and R. M. May, J. Theor. Biol. **179**, 1 (1996).
[4] N. T. J. Bailey, *The Mathematical Theory of Infectious Diseases and its Applications* (Griffin, London, 1975).
[5] R. M. Anderson and R. M. May, *Infectious Diseases of Humans* (Oxford University Press, Oxford, 1991).
[6] F. A. Milner and A. J. Pugliese, J. Math. Biol. **39**, 471 (1999).
[7] M. Altmann, J. Math. Biol. **33**, 661 (1995); M. Kretzchmar and L. G. Wiessing, AIDS **12**, 801 (1998).
[8] L. M. Wein, S. A. Zenios, and M. A. Nowak, J. Theor. Biol. **185**, 15 (1997).
[9] L. M. Wein, R. M. D'Amato, and A. S. J. Perelson, J. Theor. Biol. **192**, 81 (1998).
[10] H. C. Tuckwell and F. Y. M. Wan, IMA J. Math. Appl. Med. Biol. **17**, 311 (2000).
[11] J. D. Murray, *Mathematical Biology* (Springer, Berlin, 1993).
[12] A. Johansen, J. Theor. Biol. **178**, 45 (1996).
[13] F. Carrat, A. Flahault, E. Boussard *et al.*, J. Epidemiol. Community Health **52**, 32S (1998).
[14] J. L. Cardy, J. Phys. A **16**, L709 (1983).
[15] N. Boccara and K. Cheong, J. Phys. A **25**, 2447 (1992); B. Schonfisch, Physica D **80**, 433 (1995); C. J. Rhodes and R. M. J. Anderson, J. Theor. Biol. **180**, 125 (1996).
[16] D. Mollison, J. R. Stat. Soc. Ser. B. Methodol. **39**, 283 (1977).